Elastic and adhesive properties of alkanethiol self-assembled monolayers on gold

Frank W. DelRio,[a] Cherno Jaye, Daniel A. Fischer, and Robert F. Cook
Ceramics Division, Materials Science and Engineering Laboratory, National Institute of Standards and Technology, Gaithersburg, Maryland 20899, USA

(Received 3 February 2009; accepted 11 March 2009; published online 1 April 2009)

Elastic and adhesive properties of alkanethiol $[CH_3(CH_2)_{n-1}SH]$ self-assembled monolayers on gold are investigated by atomic force microscopy and correlated with surface structure via near edge x-ray absorption fine structure spectroscopy. As the chain length n decreases from 18 to 5, the elastic modulus of the monolayer film, E_{film}, decreases from 1.0 to 0.15 GPa and the work of adhesion, w, increases from 82.8 to 168.3 mJ m^{-2}. The E_{film} and w trends are interpreted in terms of the dichroic ratios, R_I, which reveal distinct changes in chain orientation, order, and coverage over the range of n. © *2009 American Institute of Physics*. [DOI: 10.1063/1.3111440]

Self-assembly of surfactant molecules on solid surfaces to form organic monolayer films has proven to be a convenient method to tailor the physical and chemical properties of metals, oxides, and semiconductors.[1,2] In particular, self-assembled monolayers (SAMs) prepared from thiol-terminated molecules have shown potential for use as protective layers to slow oxidation,[3] photoresistive layers for lithography,[4] receptor sites in DNA detection,[5] and charge injection barriers in organic field-effect transistors.[6] In addition, thiol-based monolayers have been used as passive[7] and active[8] molecular boundary lubricants, which provide many benefits in the operation of magnetic storage devices and microelectromechanical systems (MEMS), including a dramatic reduction in adhesion as well as enhanced lubrication.[9,10] In order to extend the usage of SAMs—particularly to magnetic storage devices and MEMS with contacting parts—methods for measuring layer mechanical properties and correlating these with layer structure are critical.

The orientation and order of methyl-terminated alkanethiols $[CH_3(CH_2)_{n-1}SH$, denoted by C_n, where n is the number of carbon atoms in the molecular chain] have been studied by a variety of techniques. Infrared spectroscopy and contact angle studies have shown that the structure and wetting properties of long-chain ($n \geq 9$) alkanethiols are independent of n, but vary greatly as n decreases.[11,12] These observations have been explained by electron diffraction studies, which indicate that long-chain alkanethiols form densely packed crystallinelike monolayers with $(\sqrt{3} \times \sqrt{3})R30°$ molecular periodicity,[13,14] while short-chain alkanethiols result in loosely packed liquidlike films with $(m\sqrt{3} \times \sqrt{3})R30°$ surface structure (where m varies from 1 to 6 depending on n).[14] While the orientation and order of alkanethiol monolayers have been well characterized, their influence on the elastic and adhesive behavior of the films is still a matter of debate. As an example, reported values for film modulus range from 0.18 to 75 GPa,[15–20] with some studies suggesting the value is independent of n (Ref. 17) and others suggesting distinct changes with n.[20] In this letter, the elastic and adhesive properties of alkanethiols on Au (n=5, 8, 12, and 18) are examined via atomic force microscopy (AFM) and correlated with surface structure by near edge x-ray absorption fine structure (NEXAFS) spectroscopy. AFM contact data are analyzed with the Derjaguin–Muller–Toporov (DMT) contact model,[21] modified to extract film modulus by a first-order elastic perturbation method to account for substrate effects.[22] NEXAFS C K-edge spectra are used to compute the dichroic ratio for each film, which provides a quantitative measure of the film structure. Taken together, these measurement techniques provide insight into the link between mechanical properties and molecular orientation, order, and coverage.

Si(100) substrates were coated with a 5 nm Ti adhesion layer followed by a 100 nm Au film. The Au-coated Si samples were cleaned in piranha solution, immersed in 1 mM ethanolic solutions of the alkanethiols for 24 h, rinsed in pure ethanol, and dried under a N_2 flow. Average values for film thickness, t, for n=5, 8, 12, and 18 were found by spectroscopic ellipsometry to be 0.38, 0.74, 1.25, and 2.03 nm, respectively, assuming a refractive index of n_f=1.50.[23] After storage in an ultrahigh vacuum (UHV) chamber for at least a week to allow for monolayer diffusion and ripening,[24] UHV AFM experiments were performed with a Si cantilever coated with 60 nm of Co followed by 20 nm of Cr. The cantilever spring constant in the normal direction was k =2.3 N m^{-1} from the thermal fluctuation method.[25] Force-deformation (F-δ) data were derived from the raw force-displacement (F-d) curves by subtracting the cantilever deflection. NEXAFS measurements were carried out at the NIST U7A beamline of the National Synchrotron Light Source. Partial electron yield (PEY) spectra at the C K-edge were obtained with a channeltron retarding voltage of −225 V to enhance the surface sensitivity and Auger yield. NEXAFS spectra were recorded at angles, θ, ranging from 20° to 90°, measured between the sample surface and the photon beam.

AFM F-δ data (unloading curves only) for n=5, 8, 12, and 18 are shown in Fig. 1. As recovered displacements are elastic on unloading, Young's modulus, E_{film}, and work of adhesion, w, of the film can be extracted from the F-δ curves with the DMT contact model, which uses a "thermodynamic approach" to include molecular adhesive forces in the contact response of a sphere of radius, R (taken as the tip radius,

[a]Author to whom correspondence should be addressed. Electronic mail: frank.delrio@nist.gov.

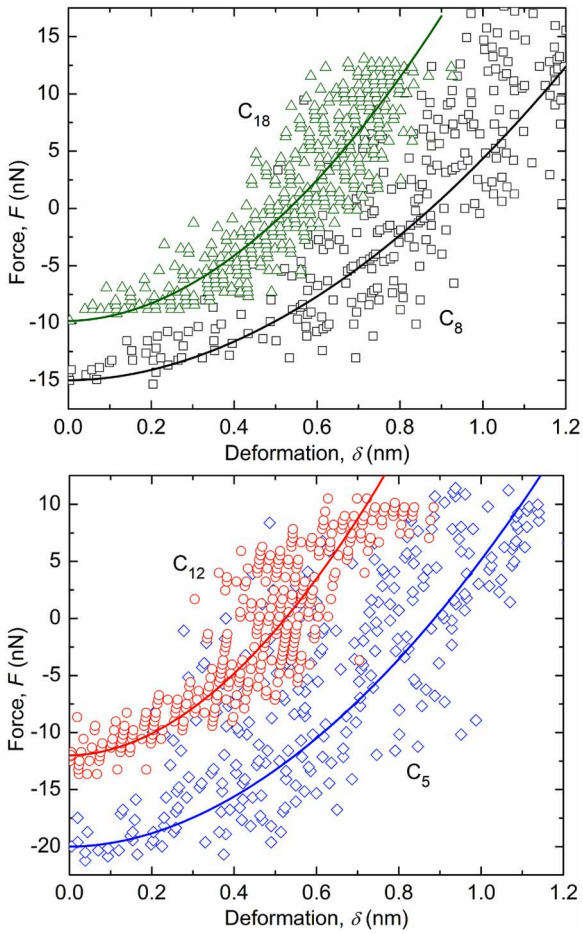

FIG. 1. (Color online) AFM F-δ data (symbols) and theoretical fits (solid lines) for n=5, 8, 12, and 18. Theoretical fits were based on an extended DMT contact model, using the modulus of the film E_{film} as the fitting parameter.

$R \approx 20$ nm), against a flat surface. In this approach, the profile of the sphere is assumed to be Hertzian with a contact radius, $a=(\delta R)^{1/2}$, and a pull-off force of $2\pi Rw$, yielding[21]

$$F = \tfrac{4}{3}E^* R^{1/2}\delta^{3/2} - 2\pi Rw, \tag{1}$$

where E^* is the reduced modulus of the contact. For a film-substrate composite, E^* is a function of the Young's moduli and Poisson's ratios of the film $(E_{\text{film}}, \nu_{\text{film}})$ *and* substrate $(E_{\text{sub}}, \nu_{\text{sub}})$. Xu and Pharr[22] developed an analytical solution for E^* of a film-substrate composite based on a first-order elastic perturbation method, which yields

$$\frac{1}{E^*} = \tfrac{1}{2}[1 - \nu_{\text{sub}} + (\nu_{\text{sub}} - \nu_{\text{film}})I_1]\left[\frac{2(1+\nu_{\text{sub}})}{E_{\text{sub}}}(1 - I_0) + \frac{2(1+\nu_{\text{film}})}{E_{\text{film}}}I_0\right], \tag{2}$$

where I_0 and I_1 are weighting functions that account for shear modulus mismatch and Poisson's ratio effects, respectively, and depend on the normalized film thickness, t/a. Values of E_{sub}=77 GPa and ν_{sub}=0.42 for the Au substrate[26] and ν_{film}=0.44 for the monolayer film[27] were used. To find w, Eq. (1) was solved at δ=0, which results in $w = -F_{\text{po}}/2\pi R$, where F_{po} is the pull-off force from each F-δ data set. In addition, Eqs. (1) and (2) were fit to the F-δ traces as shown in Fig. 1, using E_{film} as the fitting parameter.

TABLE I. Work of adhesion, Young's modulus, and C–H σ^* dichroic ratio for n=5, 8, 12, and 18.

Chain length, n	Work of adhesion,[a] w (mJ m^{-2})	Young's modulus,[a] E_{film} (GPa)	Dichroic ratio,[a] R_{I}
5	168.3 ± 17.6	0.15 ± 0.04	0.04 ± 0.04
8	125.4 ± 9.0	0.28 ± 0.08	0.02 ± 0.02
12	104.1 ± 9.8	0.86 ± 0.14	0.26 ± 0.02
18	82.8 ± 9.0	1.00 ± 0.18	0.50 ± 0.03

[a]Uncertainty values represent two standard deviations from at least five measurements or a 95% confidence level in the fit.

The values for w and E_{film} are given in Table I. Using these values, the tip radius, and the equilibrium separations from Fig. 1, the Tabor parameter[28] $\mu \approx 0.3$ for all n, justifying use of the DMT model.

NEXAFS PEY spectra at the C K-edge for n=5, 8, 12, and 18 at θ=20° and 70° are shown in Fig. 2(a). All spectra exhibit the same characteristic hydrocarbon resonance peaks: the C=C π^* peak at 285.5 eV, the C–H σ^* peak at 288.6 eV, and the C–C σ^* peak at 293.6 eV. For n=5 and 8, the spectra are nearly identical. However, n=12 and 18 reveal a strong angular dependence, with C–H σ^* resonance decreasing and

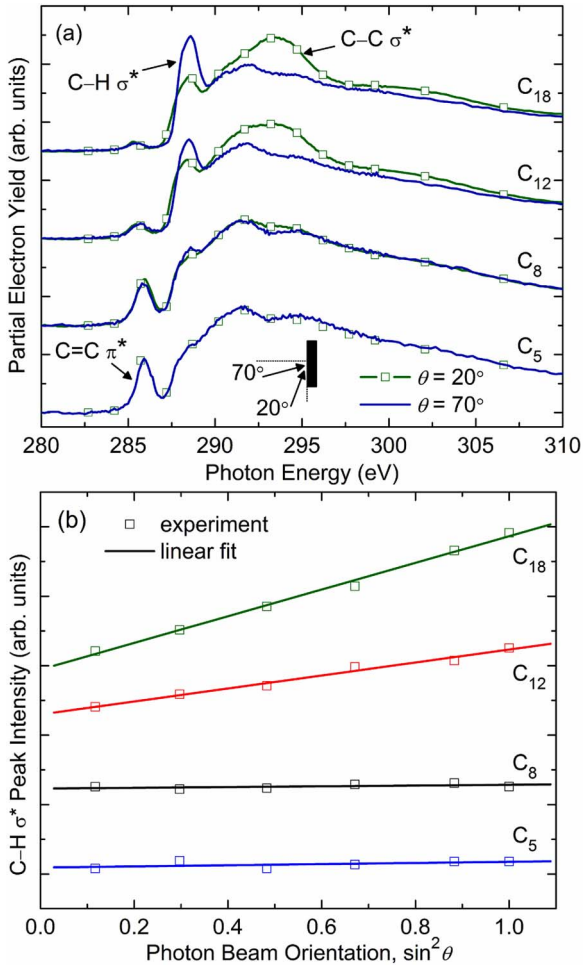

FIG. 2. (Color online) (a) NEXAFS C K-edge PEY spectra for n=5, 8, 12, and 18 at θ=20° (solid curve with symbols) and θ=70° (solid curve). (b) NEXAFS C–H σ^* peak intensities vs $\sin^2\theta$ for n=5, 8, 12, and 18 (offset for clarity). Dichroic ratios R_I were calculated using the peak intensity at θ=90° and extrapolated peak intensity at θ=0°.

C–C σ^* resonance increasing as θ decreases. In addition, as n decreases, the intensity of the C=C π^* resonance peak increases, likely the result of small surface coverage and the subsequent deposition of adventitious hydrocarbons on the Au surface for the short-chain molecules. Peak intensities were quantified by fitting Gaussian peaks to the spectra and integrating the peak areas;[29] the resulting C–H σ^* peak intensities are plotted as a function of $\sin^2\theta$ as shown in Fig. 2(b). The variations in peak intensity with θ are related to the molecular orientation through the dichroic ratio $R_I=(I_{90^\circ}-I_{0^\circ})/(I_{90^\circ}+I_{0^\circ})$, where I_{90° is the peak intensity at $\theta=90^\circ$ and I_{0° is the extrapolated peak intensity at $\theta=0^\circ$. R_I can vary from -1 to +0.75, with a more positive value for the C–H σ^* plane corresponding to greater surface normality ($R_I=0$ may also represent a random distribution of chain orientations).[30] Table I summarizes the C–H σ^* dichroic ratios. For $n=18$, $R_I=0.50$, consistent with electron diffraction studies that show a densely packed crystallinelike film.[13,14] As n decreases, R_I decreases; by definition, this indicates an increase in *average* tilt angle and change in phase from crystalline to amorphous.

From Table I, it is clear that w increases as n decreases. Berger *et al.*[31] noted a similar trend with liquid-condensed (LC) and liquid-expanded (LE) domains in a phase-separated lipid monolayer. The change was attributed to differences in molecular orientation and order; in the LC domains, the molecules were densely packed and the probe tip interacted only with the CH_3 end groups, whereas in the LE domains, the films were liquidlike and the adhesion was mainly due to CH_2 groups along the hydrocarbon chain. With $\gamma_{CH2}=31$ mJ m^{-2} and $\gamma_{CH3}=23$ mJ m^{-2}, they found $w_{CH2}/w_{CH3}=(\gamma_{CH2}/\gamma_{CH3})^{1/2}=1.2$, where γ_a and w_a are the surface energy and work of adhesion for molecule a, respectively. Seeing that the average tilt angle increases as n decreases, as shown by the trends in R_I, a similar increase in work of adhesion should be expected here due to the additional CH_2 groups at the surface. Koleske *et al.*[32] showed that the elastic modulus of a film may also affect tip-surface interactions. As E_{film} decreases, δ at a given F increases, which exposes the tip to additional functional groups in the film or to the substrate. As shown in Table I, E_{film} decreases from 1.0 to 0.15 GPa as n decreases from 18 to 5, which might further explain the larger values of w for the short-chain molecules.

The variation in E_{film} with n can be divided into three regions, each the result of a different variation mechanism, but which all derive from the variation in the attractive van der Waals interactions between alkyl chains with n.[33] As n increases for densely packed chains, the stabilization energy provided by additional CH_2 groups decreases, and eventually saturates at $n\approx 10$. Hence, the small decrease in E_{film} as n decreased from 18 to 12 arises from a decrease in n. For n decreasing from 12 to 8, E_{film} decreased by an additional factor of 3. In this range the intermolecular forces are no longer invariant with n, but decrease as n decreases, resulting in a greater concentration of *gauche* defects along the chains. As a consequence, the film becomes more disordered (as indicated by $R_I\rightarrow 0$), which reduces its resistance to elastic deformation. For $n<8$, a lack of cohesive energy leads to the thermal desorption of alkyl chains at low-energy sites on the surface[34] (as indicated by the increase in C=C π^* peak intensity) and the loss of surface coverage leads to the decrease in E_{film} over this range. Overall, the results for E_{film} are in agreement with a number of previous studies for both polyethylene (0.172–1.08 GPa)[26] and alkanethiol monolayers (0.18–5 GPa).[15,16,18,19] Reports of much greater moduli for organic monolayers, from 15 to 75 GPa,[17,20] are probably due to the imposed boundary conditions[17] or substrate effects,[20] corrected here through the use of Eq. (2).

In summary, the elastic and adhesive properties of alkanethiol monolayers on Au were examined with AFM and correlated with surface structure via NEXAFS. The combination of the two measurement methods—building on an extension of the contact method to extract the film modulus—provides a structure-property relationship for this particular system and a general methodology for the optimization of SAMs for MEMS, magnetic storage, and other applications.

[1] A. Ulman, Chem. Rev. (Washington, D.C.) **96**, 1533 (1996).
[2] D. K. Schwartz, Annu. Rev. Phys. Chem. **52**, 107 (2001).
[3] P. E. Laibinis and G. M. Whitesides, J. Am. Chem. Soc. **114**, 9022 (1992).
[4] V. C. Sundar and J. Aizerberg, Appl. Phys. Lett. **83**, 2259 (2003).
[5] M. Su, S. Li, and V. P. Dravid, Appl. Phys. Lett. **82**, 3562 (2003).
[6] K. Asadi, F. Gholamrezaie, E. C. P. Smits, P. W. M. Blom, and B. de Boer, J. Mater. Chem. **17**, 1947 (2007).
[7] S. T. Patton, K. C. Eapen, J. S. Labinski, J. H. Sanders, and A. A. Voevodin, J. Appl. Phys. **102**, 024903 (2007).
[8] J. Lahann, S. Mitragotri, T.-N. Tran, H. Kaido, J. Sundaram, I. S. Choi, S. Hoffer, G. A. Somorjai, and R. Langer, Science **299**, 371 (2003).
[9] A. M. Homola, IEEE Trans. Magn. **32**, 1812 (1996).
[10] R. Maboudian and R. T. Howe, J. Vac. Sci. Technol. B **15**, 1 (1997).
[11] M. D. Porter, T. B. Bright, D. L. Allara, and C. E. D. Chidsey, J. Am. Chem. Soc. **109**, 3559 (1987).
[12] C. D. Bain, E. B. Troughton, Y.-T. Tao, J. Evall, G. M. Whitesides, and R. G. Nuzzo, J. Am. Chem. Soc. **111**, 321 (1989).
[13] L. Strong and G. M. Whitesides, Langmuir **4**, 546 (1988).
[14] L. H. Dubois, B. R. Zegarski, and R. G. Nuzzo, J. Chem. Phys. **98**, 678 (1993).
[15] M. Salmeron, G. Neubauer, A. Folch, M. Tomitori, D. F. Ogletree, and P. Sautet, Langmuir **9**, 3600 (1993).
[16] W. Kiridena, V. Jain, P. K. Kuo, and G. Liu, Surf. Interface Anal. **25**, 383 (1997).
[17] R. Henda, M. Grunze, and A. J. Pertsin, Tribol. Lett. **5**, 191 (1998).
[18] J. E. Houston and H. I. Kim, Acc. Chem. Res. **35**, 547 (2002).
[19] W. J. Price, S. A. Leigh, S. M. Hsu, T. E. Patten, and G. Liu, J. Phys. Chem. A **110**, 1382 (2006).
[20] V. B. Engelkes and C. D. Frisbie, J. Phys. Chem. B **110**, 10011 (2006).
[21] B. V. Derjaguin, V. M. Muller, and Y. P. Toporov, J. Colloid Interface Sci. **53**, 314 (1975).
[22] H. Xu and G. M. Pharr, Scr. Mater. **55**, 315 (2006).
[23] A. Ulman, *An Introduction to Ultrathin Organic Films: From Langmuir-Blodgett to Self-Assembly* (Academic Press, New York, 1991).
[24] E. Barrena, C. Ocal, and M. Salmeron, J. Chem. Phys. **111**, 9797 (1999).
[25] J. L. Hutter and J. Bechhoefer, Rev. Sci. Instrum. **64**, 1868 (1993).
[26] W. D. Callister, *Materials Science and Engineering: An Introduction* (Wiley, New York, 2000).
[27] M. Wang, K. M. Liechti, V. Srinivasan, J. M. White, P. J. Rossky, and M. T. Stone, ASME J. Appl. Mech. **73**, 769 (2006).
[28] D. Tabor, J. Colloid Interface Sci. **58**, 2 (1977).
[29] D. A. Outka, J. Stöhr, J. P. Rabe, and J. D. Swalen, J. Chem. Phys. **88**, 4076 (1988).
[30] S. Sambasivan, S. Hsieh, D. A. Fischer, and S. M. Hsu, J. Vac. Sci. Technol. A **24**, 1484 (2006).
[31] C. E. H. Berger, K. O. van der Werf, R. P. H. Kooyman, B. G. de Grooth, and J. Greve, Langmuir **11**, 4188 (1995).
[32] D. D. Koleske, W. R. Barger, G. U. Lee, and R. J. Colton, Mater. Res. Soc. Symp. Proc. **464**, 377 (1997).
[33] X. Xiao, J. Hu, D. H. Charych, and M. Salmeron, Langmuir **12**, 235 (1996).
[34] R. G. Nuzzo, B. R. Zegarski, and L. H. Dubois, J. Am. Chem. Soc. **109**, 733 (1987).